CHEMISTRY
A European Journal

Supporting Information

Formation of the Charge-Localized Dimer Radical Cation of 2-Ethyl-9,10-dimethoxyanthracene in Solution Phase

Jungkweon Choi[+,[a, b]] Doo-Sik Ahn[+,[a, b]] Mamoru Fujitsuka,[c] Sachiko Tojo,[c] Hyotcherl Ihee,*[a, b] and Tetsuro Majima*[c]

chem_201900175_sm_miscellaneous_information.pdf

Supplementary Information

List of contents

Table S1. DFT and TD-DFT Calculated energies, C_9-C_9(C_{10}) distance, and near-IR transitions of $(DMA)_2^{\bullet+}$

	Energy (hartree)	ΔE (kcal mol^{-1})	R(C-C) (Å)	Near-IR transition energy (nm)	Oscillator strength
B3LYP/6-31G(d)					
$DF1^{\bullet+}$	-1694.224222	1.4	3.545	2227	0.1043
$DF2^{\bullet+}$	-1694.223997	1.5	3.566	2282	0.1146
$DF3^{\bullet+}$	-1694.226402	0.0	3.443	1870	0.1156
$DT^{\bullet+}$	-1694.220005	4.0	8.242	3270	0.0004
$CDF^{\bullet+}$	-1694.117001	68.6	1.689	N/A*	N/A
B3LYP/6-31+G(d,p)					
$DF1^{\bullet+}$	-1694.317177	1.2	4.008	3498	0.0655
$DF2^{\bullet+}$	-1694.316615	1.5	3.745	2815	0.0899
$DF3^{\bullet+}$	-1694.319016	0.0	3.732	2474	0.0914
$DT^{\bullet+}$	-1694.316119	1.8	8.347	2785	0.0004
$CDF^{\bullet+}$	-1694.207665	69.9	N/A	N/A	N/A
CAM-B3LYP/ 6-31+G(d,p)					
$DF1^{\bullet+}$	-1693.385669	2.8	3.272	3593	0.1416
$DF2^{\bullet+}$	-1693.384615	3.4	3.310	4016	0.1466
$DF3^{\bullet+}$	-1693.390085	0.0	3.628	1462	0.0458
$DT^{\bullet+}$	-1693.389396	0.4	7.759	786	0.0
M06-2X/6-31+G(d,p)					
$DF1^{\bullet+}$	-1693.584212	2.2	3.347	1900	0.0367
$DF2^{\bullet+}$	-1693.579136	5.4	3.018	2007	0.1501
$DF3^{\bullet+}$	-1693.587728	0.0	2.998	1719	0.1302

*N/A: not available

Figure S1. a) Transient absorption spectra of DMA (0.5 mM) in DCE observed at various times after pulse radiolysis by an 8-ns electron pulse. Inset: expanded view of the near-IR transient absorption spectra b) Decay profiles monitored at 550 (black) and 1300 nm (blue).

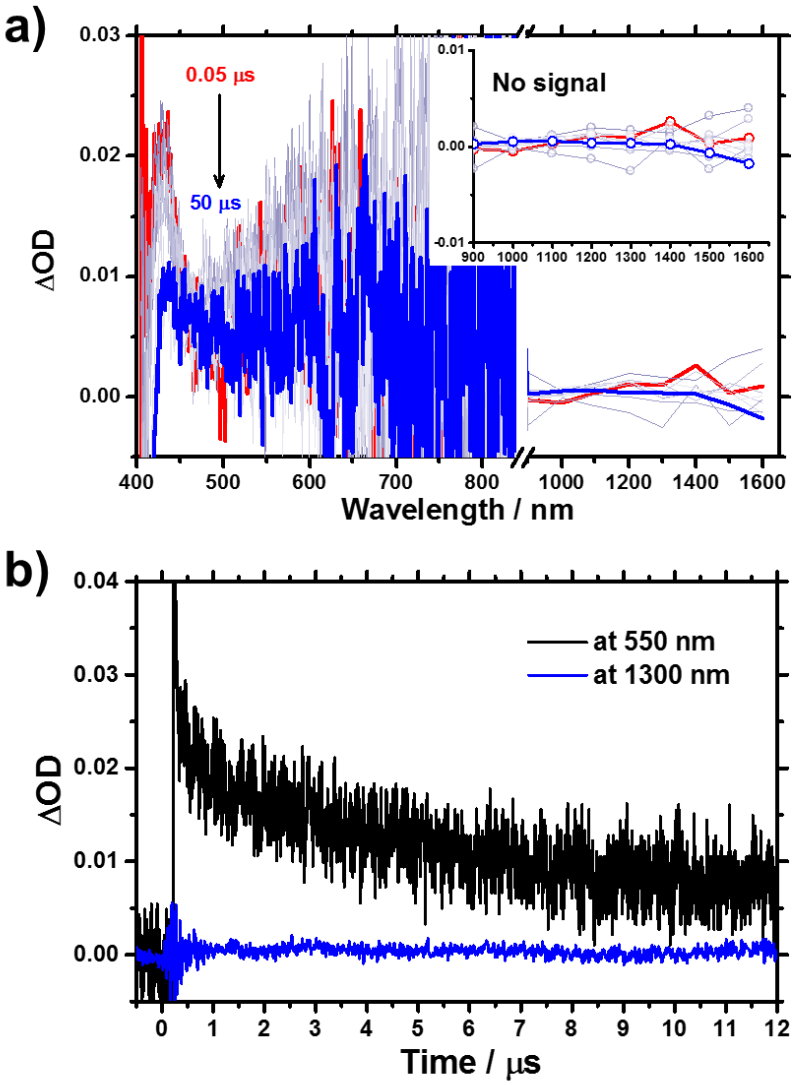

Figure S2. a) Transient absorption spectra of DMA (5 mM) in DCE observed at various times after pulse radiolysis by an 8-ns electron pulse. Inset: expanded view of the near-IR transient absorption spectra b) Decay profiles monitored at 550 (black) and 1300 nm (blue).

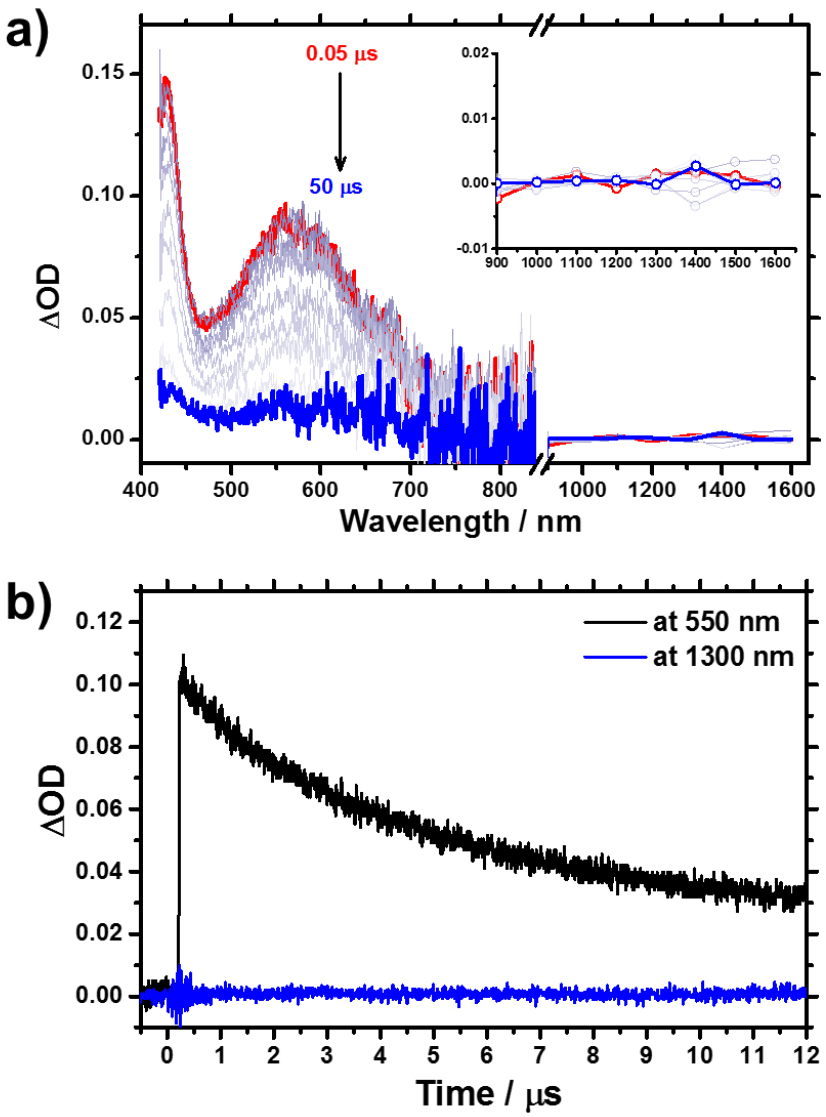

Figure S3. a) Transient absorption spectra of DMA (50 mM) in DCE observed at various times after pulse radiolysis by an 8-ns electron pulse. Inset: expanded view of the near-IR transient absorption spectra b) Decay profiles monitored at 550 (black) and 1300 nm (blue).

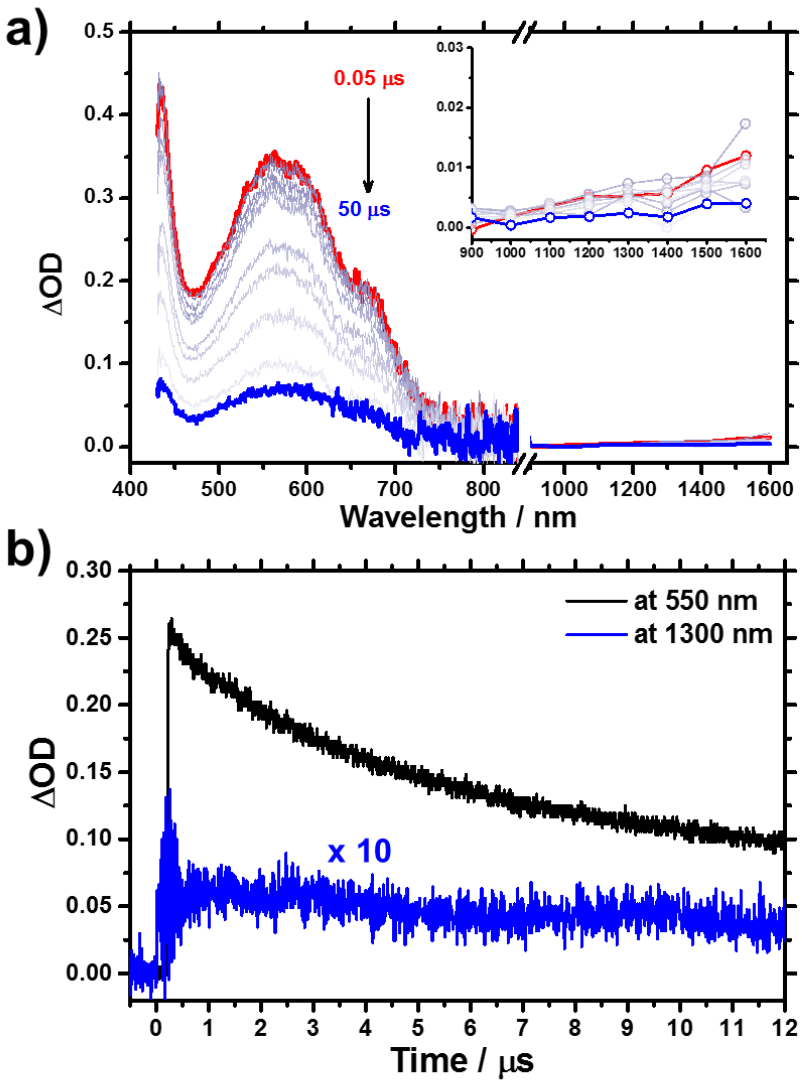

Figure S4. a) Transient absorption spectra observed at 50 ns after pulse radiolysis by an 8 ns electron pulse as a function of the DMA concentration. b) Decay profiles monitored at 550 nm.

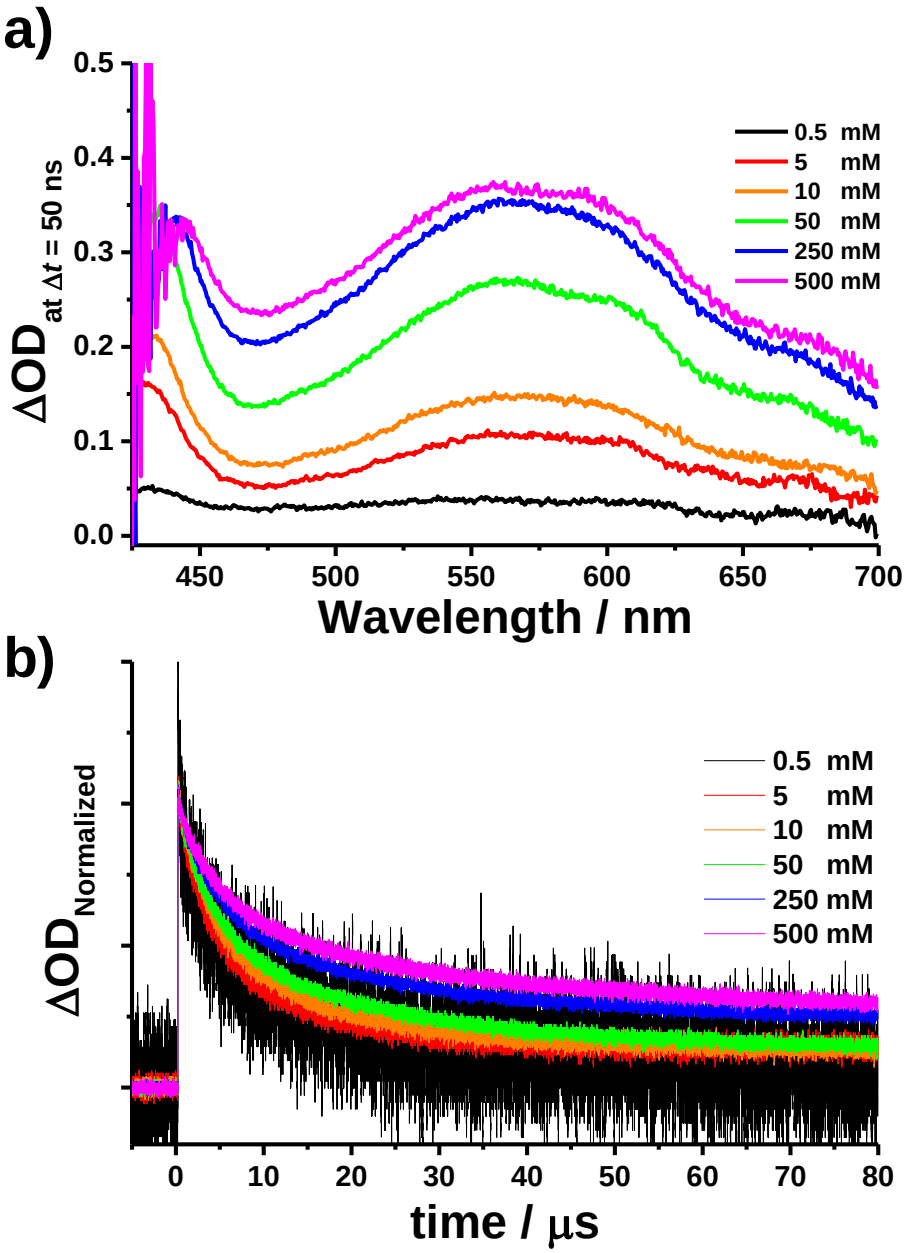

Figure S5. a) Decay profile monitored at 1300 nm (blue). The theoretical fit curve is represented by the solid red line. b) Residual of global fit with a rise component. c) Residual of global fit using without a rise component.

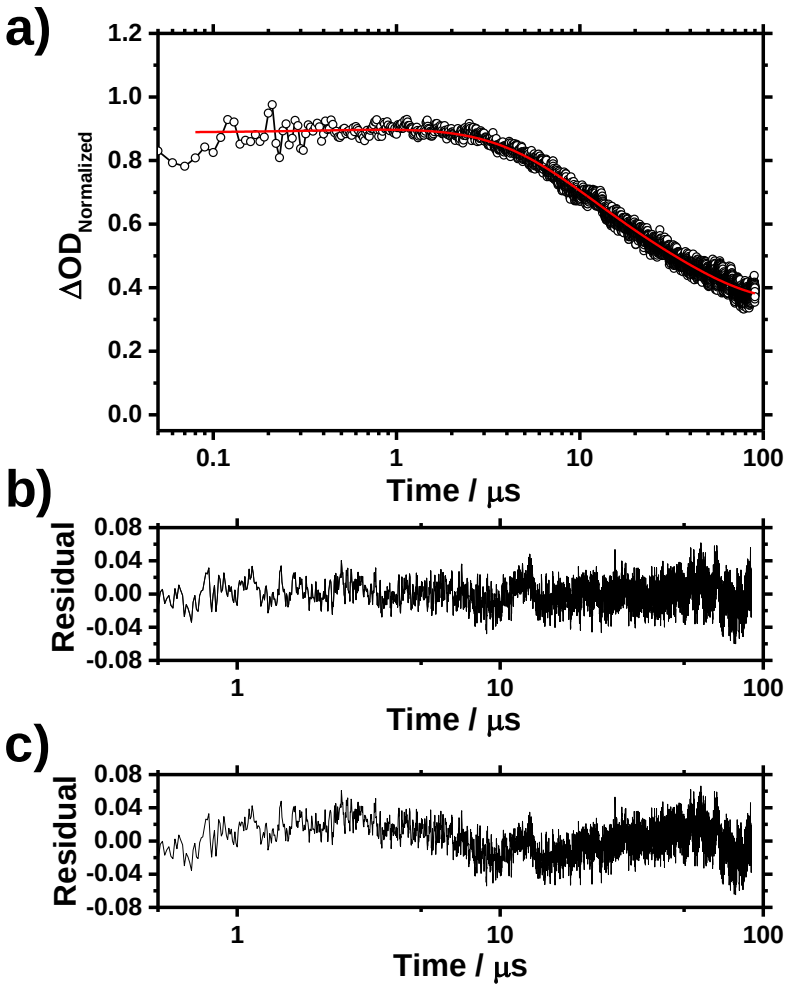

Figure S6. Enlarged views of TR^3 spectra at the main peaks around 1300 (a) and 1415 (b) cm^{-1}.

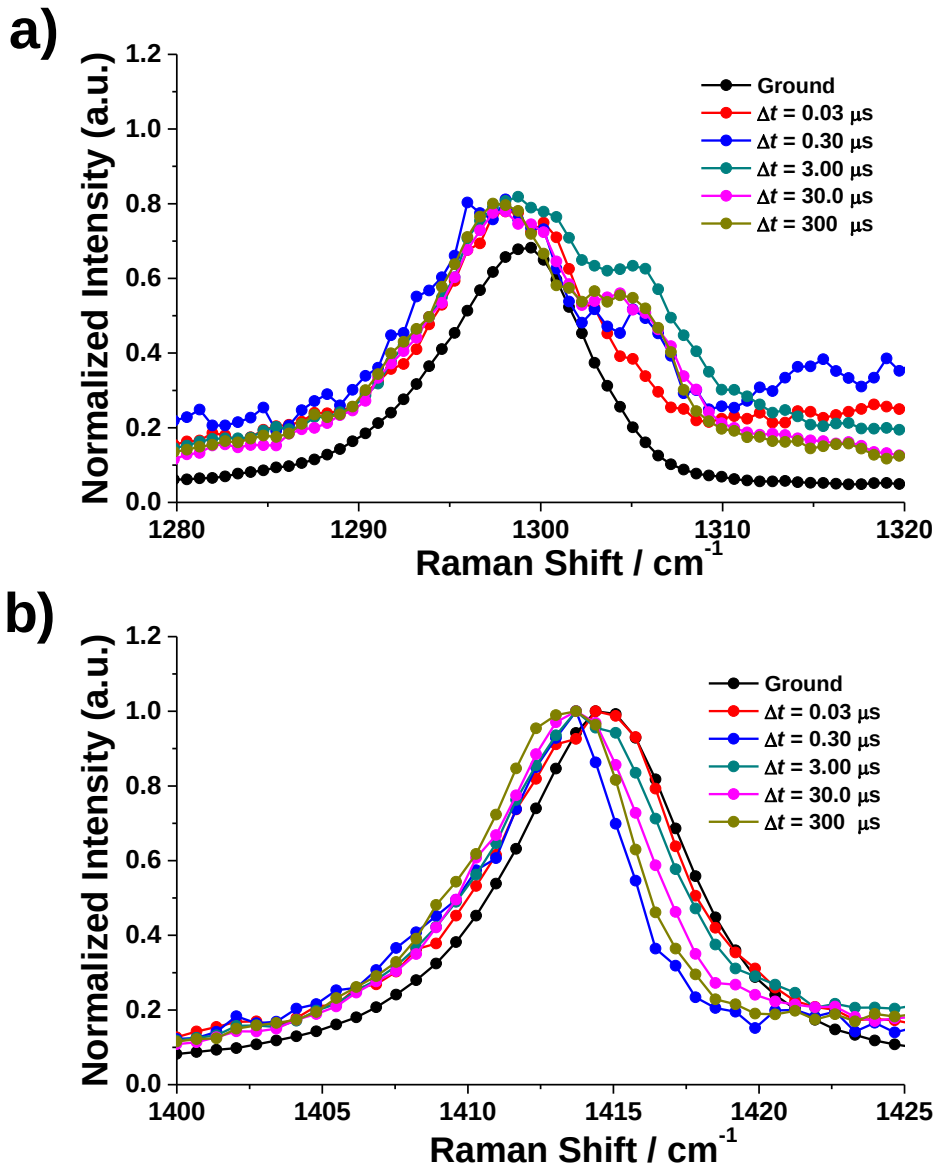

Figure S7. Normalized TR^3 spectra of DMA observed at various time delays after pulse radiolysis.

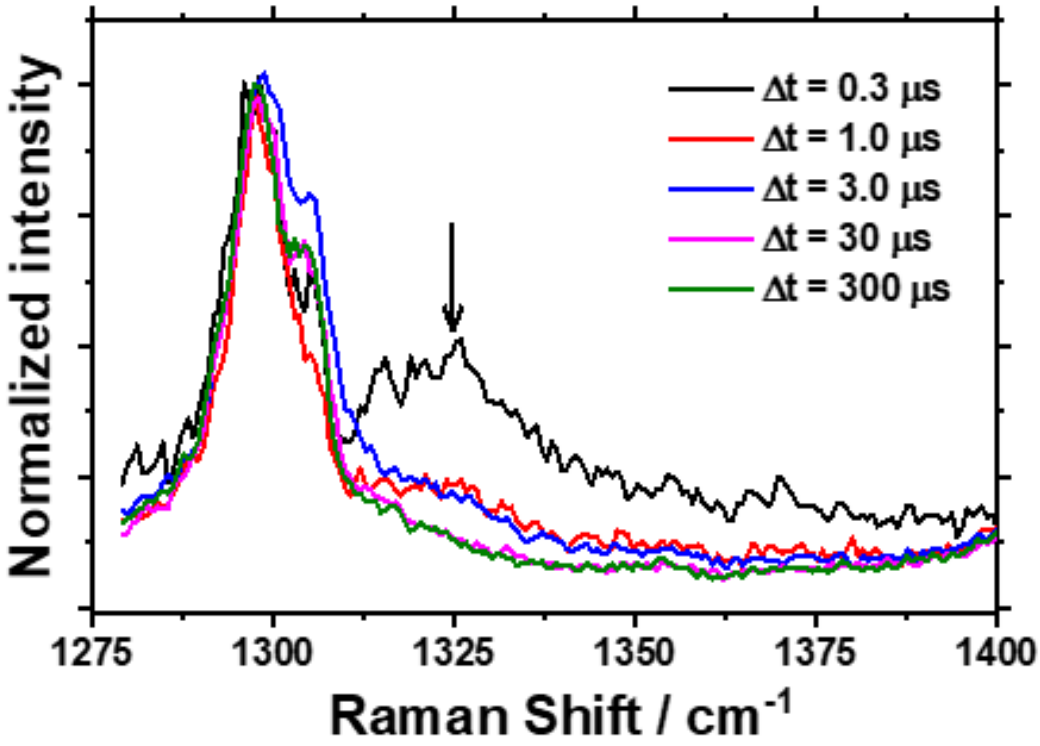

Figure S8. a) Calculated structures of *trans*- and *cis*-conformers of DMA and DMA$^{\bullet+}$ b) Calculated barrier heights (kcal mol^{-1}) for single *rotation of methoxy* group in DMA and DMA$^{\bullet+}$.

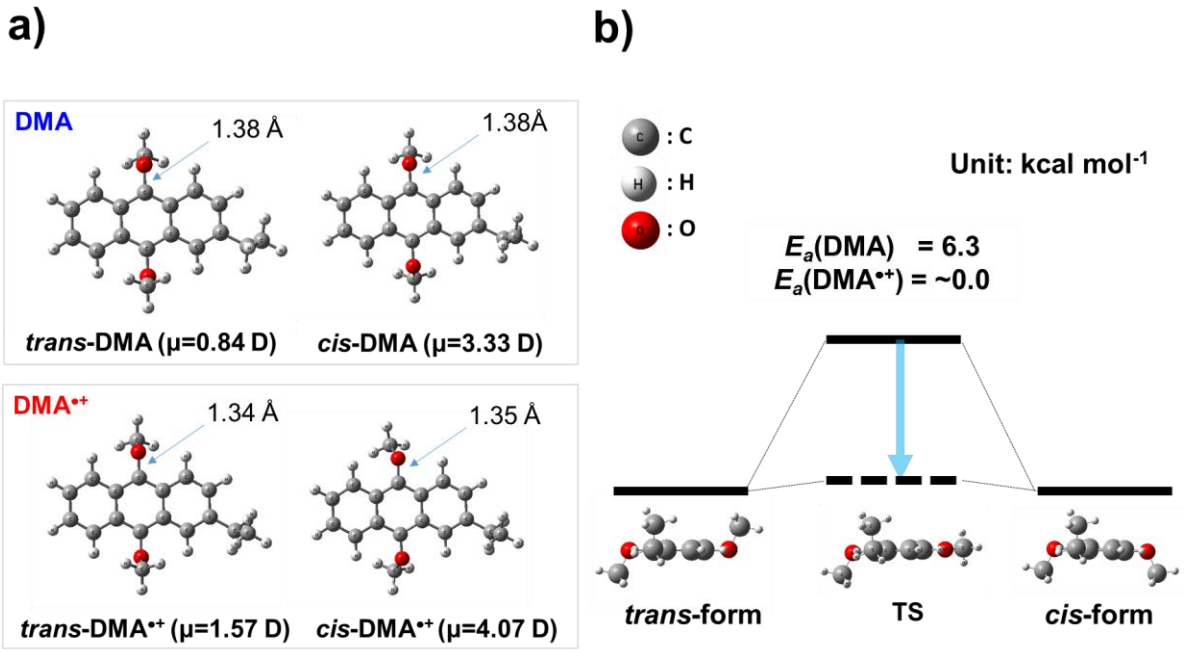

Figure S9. Top panel) TA spectra of DMA (250 mM) in DCE observed at 100 ns and 50 µs after pulse radiolysis by an 8-ns electron pulse. Middle panel) Calculated transition wavelengths and oscillator strengths for $DMA^{\bullet+}$ and $(DMA)_2^{\bullet+}$ using B3LYP/6-31+G(d,p). Bottom panel) Calculated transition wavelengths and oscillator strengths for $DMA^{\bullet+}$ and $(DMA)_2^{\bullet+}$ using M06-2X/6-31+G(d,p).